MODELLING OF FATIGUE STRENGTH DATA FOR A SHORT FIBRE REINFORCED POLYAMIDE 6.6 BASED ON LOCAL STRAIN ENERGY DENSITY

M. De Monte*, M. Quaresimin, P. Lazzarin****
***Robert Bosch GmbH - Corporate Research (CR/APP2), Waiblingen (Germany)**
****Department of Management and Engineering – University of Padova (Italy)**

Keywords: *fatigue strength, strain energy density, short fiber reinforced plastics, energetic failure criterion, notch effect, control radius, polyamide 6.6*

Abstract

This paper presents the application of an energetic approach to assess the fatigue behaviour of a short fibre reinforced polyamide PA66-GF35 under uniaxial loading. Fatigue data of specimens with five different notch radii ρ (80, 5, 1, 0.5 and 0.2 mm) and two load ratios (R=0 and R=-1) are reanalysed in terms of strain energy density (SED) at room temperature as well as 130°C. Nominal SED, elastic peak SED and an average SED are compared. In the last case the strength reduction due to notches is accounted by averaging the SED over a control volume, defined by a material specific critical radius R_C. This procedure is implemented in a python script to post-process structural simulation results. The material is modelled as transverse isotropic, assuming a unidirectional fibre alignment. The advantages and the limitations of the proposed approach for short fibre reinforced plastics are discussed.

1 Introduction

Fatigue strength assessment of structural components requires a failure criterion applicable to blunt as well as sharp notches, to uniaxial as well as multiaxial loading and to every given load ratio. The failure criteria should need only few experimental data to be validated and possibly be easy to implement in finite element codes for practical application on components.

Criteria based on strain energy density (SED) have been successfully applied to metals [1], [2] and unnotched composites [3] under fatigue loading, and to quasi-brittle materials under static loading [1], [4].

Energetic failure criteria are empirical, they do not consider damage mechanics parameters directly connected to fatigue damage. The SED is always positive and practically insensitive to the stress component sign, so that tensile and compressive loadings are considered equivalent in terms of energy; the critical SED value instead depends in general on the load ratio *R*. Moreover, these criteria are suitable only to assess crack initiation and give no indication on direction and extension of crack propagation. Accounting for fatigue strength reduction due to notches is however still a controversial question, for isotropic as well as for anisotropic materials.

As concerns isotropic materials, Neuber [5] introduced a material-dependent *microstructural support length* over which the stress should be averaged to determine the stress concentration factor. Lazzarin and Zambardi [1] suggested using the mean value over a control volume of the local SED to predict fatigue behaviour of metallic components weakened by sharp V-notches with variable notch angle. Lazzarin and Berto later extended the method to blunt V-notches and U-notches [6].

Whitney and Nuismer [7], [8] developed two criteria for the ultimate tensile strength (UTS) of orthotropic laminates containing a circular opening or a straight crack. The former criterion is based on the stress at a point a fixed distance d_0 away from the notch tip (*Point Stress Criterion*), while the latter considers the average stress over some fixed distance a_0 ahead of the notch (A*verage-Stress Criterion*). Both cases assume failure to occur when the reference stress (point stress or average-stress) reaches the unnotched tensile strength of the material. Considering a particular material

configuration (i.e. laminate lay-up), the characteristic distances a_0 and d_0 are independent of notch radius or crack size, implicitly assuming that they are material constants.

Observing that circular openings and cracks are both extreme cases of ellipse-shaped openings, Tan [9], [10], [11] extended Whitney-Nuismer's *Point Stress* and *Average-Stress* criteria to the case of elliptical openings. He found out that the characteristic lengths a_0 and d_0 are both functions of the opening aspect ratio and proposed therefore a modified criterion that included the opening length and aspect ratio in the formulas for a_0 and d_0.

Zago and Springer [12] obtained good results using the Whitney-Nuismer *Point Stress Criterion* to assess the fatigue life of a coupon made of Copolyamide matrix reinforced with 50% wt. of short glass fibres, containing a 2 mm hole. They assumed the critical distance d_0 to be the same for quasi-static and cyclic loading and reported a value $d_0 = 0.2$ mm for the considered material.

In this work an average SED criterion will be extended to short fibre reinforced plastics (SFRP), reanalysing some available data on notched PA66-GF35 specimens. To the authors' knowledge, a similar approach has not been reported previously in literature and is substantially new in the field of composite materials.

2 Theoretical model

In this paper it is assumed that high-cycle fatigue failure will occur when the average SED ΔW_{avg} over a material control envelope around the notch tip reaches a critical value ΔW_c. The control envelope can be an area in case of the 2D representation or a volume is the 3D case. ΔW_{avg} is supposed to be independent of the notch-opening angle.

At a reference number of cycles to failure N (for SFRP usually it is $N = 10^6$), the critical value ΔW_c is supposed to be the nominal SED at failure of a plain specimen in the same configuration of the notched one. ΔW_c can be calculated analytically, considering the ranges of nominal stress components and the material compliance matrix components, both referring to the geometrical coordinate system *0,X,Y,Z*.

Consider a notched specimen of an orthotropic material, obeying to a linear elastic law when subjected to cyclic loading. At a generic instant t of the loading cycle, in a generic position Q around the notch tip, the SED can be written as:

$$W_Q(t) = \frac{1}{2}\left(S_{11}\sigma_1^{\,2} + S_{22}\sigma_2^{\,2} + S_{33}\sigma_3^{\,2} + \right. \\ + 2S_{12}\sigma_1\sigma_2 + 2S_{13}\sigma_1\sigma_3 + 2S_{23}\sigma_2\sigma_3 + \\ \left. + S_{44}\sigma_{12}^{\,2} + S_{55}\sigma_{13}^{\,2} + S_{66}\sigma_{23}^{\,2}\right) \quad (1)$$

S_{ij} are the compliance matrix components and σ_i and σ_{ij} the local stress components at the instant t and position Q, in the material coordinate system *0,1,2,3*. The stress distribution ahead of the notch tip can be computed analytically in some standard cases [9], [10], [11], [13] but on complex geometries and orthotropic material formulation it is generally obtained by a finite element analysis (FEA).
The local SED range under cyclic loading at the position Q can be instead written as:

$$\Delta W_Q = \frac{c_W}{2}\left(S_{11}\Delta\sigma_1^{\,2} + S_{22}\Delta\sigma_2^{\,2} + \right. \\ + S_{33}\Delta\sigma_3^{\,2} + 2S_{12}\Delta\sigma_1\Delta\sigma_2 + \\ + 2S_{13}\Delta\sigma_1\Delta\sigma_3 + 2S_{23}\Delta\sigma_2\Delta\sigma_3 + \\ \left. + S_{44}\Delta\sigma_{12}^{\,2} + S_{55}\Delta\sigma_{13}^{\,2} + S_{66}\Delta\sigma_{23}^{\,2}\right) \quad (2)$$

$\Delta\sigma_{i,n}$ and $\Delta\sigma_{ij,n}$ are the ranges of normal and shear stress components at the position Q respectively and c_w is the load ratio parameter proposed by Lazzarin *et al.* [14] to account for different R values. Equation (2) implicitly assumes that the same load ratio is applied to all load components; if this is not the case a different c_w should be used for every load component.

The control area A_C or the volume V_C, over which the SED will be averaged, is determined by a control radius R_{Con}, as the sum of a material specific critical radius R_C and by the distance R_0, which depends upon the notch geometry:

$$R_{Con} = R_0 + R_C \quad (3)$$

For isotropic materials under mode I loading and plain strain conditions Yosibash *et al.* [4] proposed the following relation to compute R_C in case of a cracked specimen:

$$R_C = \frac{(1+\nu)(5-8\nu)}{4\pi}\left(\frac{K_{IC}}{\sigma_{X,C}}\right)^2 \quad (4)$$

being ν the Poisson ratio, K_{IC} the critical stress intensity factor and $\sigma_{X,C}$ the yield stress for ductile materials and the stress at fracture for brittle materials, all expressed in the configuration system

given by the material axis *1,2* and the loading axis *X;Y*.
Equation (4) can be modified for cyclic loading using ranges instead of absolute values:

$$R_C = \frac{(1+\nu)(5-8\nu)}{4\pi}\left(\frac{\Delta K_{th}}{\Delta\sigma_{X,N,R,T}}\right) \qquad (5)$$

where ΔK_{th} is the threshold value of the stress intensity factor range and $\Delta\sigma_{X,N,R,T}$ is the specimen plain fatigue strength at the number of cycles N, load ratio R and temperature T for the considered material and load configuration.
The distance R_0, instead, can be calculated with the following relation proposed by Neuber [5]:

$$R_0 = \rho\frac{\pi - 2\alpha}{2\pi - 2\alpha} \qquad (6)$$

where ρ is the notch root radius and 2α is the notch opening angle. For U-notches it is $2\alpha = 0$, resulting in $R_0 = \rho/2$; the same value will be used for holes, considered as a particular case of U-notches.

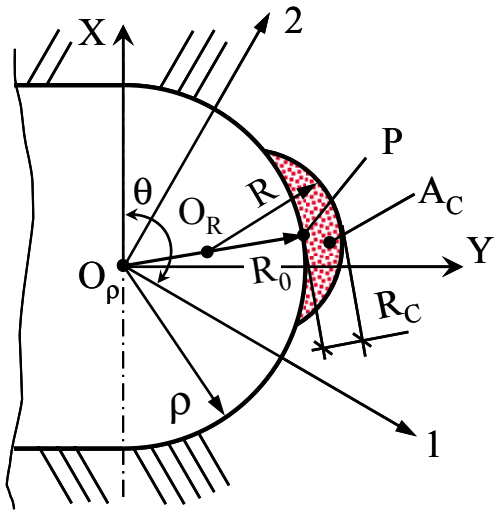

Fig. 1. Two-dimensional illustration of the material critical radius R_C, the origin radius R_0, the control radius R and the control area A_C for a U-notch

A 2D schematical representation of such a control envelope (the area A_C) in the case of an off-axis orthotropic plate with a U-notch is reported in Fig. 1. The external load is applied in the geometrical system $O_\rho X,Y$, while the material reference system is designated with $O_\rho 1,2$, being θ the off-axis angle formed by the material fist axis, i.e. fibre direction, with the geometrical axis X. P is the position of the elastic peak value of the SED, deriving from the applied load and the material configuration. Due to the material anisotropy it is not necessarily coincident with the notch tip. Anyway, the position of the SED peak is always close to the notch tip, independently of the material configuration, which is definitely not the case for the peak positions of the stress components in the material coordinate system. Once R_C and R_0 are known, i.e. from relations (5) and (6), the control radius origin O_R can be determined on the line connecting O_ρ and P.

In the 3D representation the shape of the control volume depends upon specimen geometry: for a specimen obtained by extrusion it will be a prism, for an axis-symmetric specimen it will be a toroidal volume. When a real, complex geometry is considered a portion of a sphere is the suggested shape.

3 Fatigue data

Different sets of fatigue data already published in [15] were used to assess the validity of the exposed SED based model. The datasets refer to stress-controlled fatigue data on plain and notched specimens under uniaxial loading with constant amplitude. Specimens were obtained by injection moulding of a polyamide 6.6 reinforced with 35 % wt. of short glass fibres (PA66-GF35). Fibres had a diameter of 10 µm and an average length of approximately 280 µm.

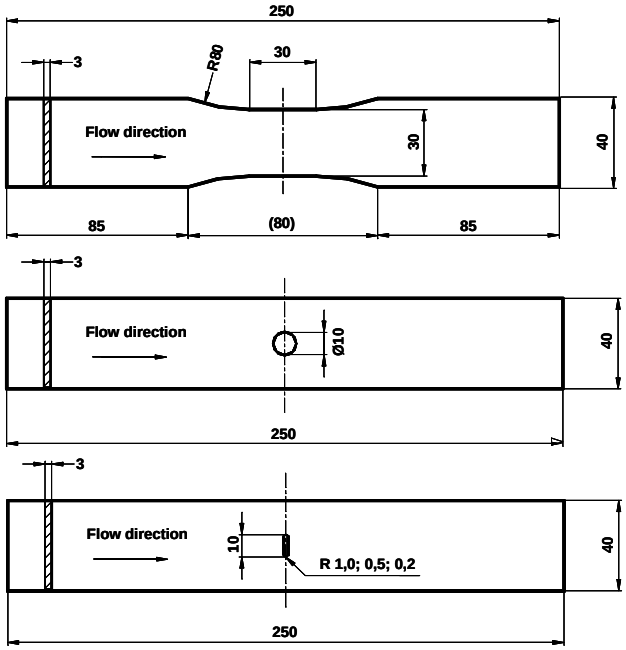

Fig. 2. Geometry of the specimens considered. All dimensions in mm.

The plain specimen had a shoulder of 80 mm radius, while among the notched specimens there was a central hole with ρ = 5 mm radius and three different central slits with radius of 1, 0.5 and 0.2 mm respectively. Except for the plain specimen, whose shoulders were machined out after injection moulding of 250 x 40 x 3 mm plates, all the notched specimens were moulded to shape, so that no secondary machining had to be performed. The geometry of the specimens is summarised in Fig. 2, where fibres are mainly aligned in flow direction. The effect of notches, load ratio, temperature, weld lines and fibre orientation has been reported in a previous investigation [15].

In the following reanalysis only the fatigue data with fibres nominally aligned in the loading direction *X* (longitudinal fibre orientation) will be considered. The data for different notch radii, load ratios R = 0 and R = -1 at room temperature (RT) and T = 130°C are reanalysed. For the tension-compression tests an anti-buckling device was applied on the specimens.

The following fatigue life model was used to describe the experimental data:

$$\Delta W(N) = \Delta W(10^6) \cdot \left(\frac{10^6}{N} \right)^{\frac{1}{k}} \qquad (7)$$

where $\Delta W(10^6)$ and k are the two fitting parameters. Rewriting eq. (7) in the logarithmic form the model becomes linear; for the fitting *log(N)* was considered as model response and *log[ΔW(N)]* as independent variable.

4.1 Structural simulations

The distribution of SED and stresses in the specimen was computed by a three dimensional FEA using the commercial software ABAQUS®. Even if the applied load was uniaxial the presence of notches induced a multiaxial stress state around the notch tip.

In the structural simulation the material was modelled as transverse isotropic linear elastic. The elastic constants were obtained from off-axis tests on 80 mm long dog-boned specimens [16]. In this investigation the elastic constants were reported to be quite sensitive to the specimen thickness, due to a different degree of fibre alignment in flow direction.

Comparing qualitatively the fibre orientation of the 250 mm long specimens considered in this modelling with that of the 80 mm long specimens used in the off-axis tests reported in [16] it was decided to adopt the elastic constants of the 1 mm thick off-axis specimens. Indeed, even if the thickness of the 250 mm specimens is 3 mm, the side walls of the mould cause a higher degree of fibre alignment in flow direction than the one obtained on the 80x80 mm plates of the same thickness, from which the off-axis specimens were machined out. The experimental elastic constants in the material reference system are reported in Table 1, where 1 designates the fibre direction and 2-3 is the plane of isotropy for the material.

Table 1. Elastic constants of PA66-GF35 from off-axis tests at RT [16]

E_1 [GPa]	E_2 [GPa]	G_{12} [GPa]	ν_{12} [-]
9.92	5.72	2.42	0.40

In order to fully describe the 3D material behaviour some assumptions have to be made to determine all components of the 3D compliance matrix.

Usually five elastic constants are used to characterise the mechanical behaviour of transverse isotropic materials. Christensen [17] demonstrated that only four elastic constant are actually required. For this kind of materials the compliance matrix can be decomposed into three parts, related to the extensional properties, the Poisson's ratio properties and to the shear properties respectively. Upon simple considerations on these matrixes, six distinct sub-classes of transverse isotropy can be identified; actually only two of the six cases are relevant to determine an unambiguous relation between the five elastic constants, namely the cases of isotropy of extensional effects and that of isotropy of Poisson ratio effects. In this work it is assumed that Poisson ratio properties are isotropic, leading to following relationship:

$$\nu_{23} = \nu_{12} \left(\frac{1 - \nu_{21}}{1 - \nu_{12}} \right) \qquad (8)$$

All other elastic constants are given by the conventional formulas of the theory of elasticity for orthotropic materials [18].

The restrictions to the elastic constants due to material stability, as reported in [19], were verified.

Quadratic hexahedral elements with reduced integration (*C3D20R* in ABAQUS) were used: each element had 20 nodes and 8 integration points. The

simulations were performed as *small displacement* analysis, considering the reference (original) configuration for strain calculations; geometric nonlinearity is ignored in the element calculations.

A very fine mesh was adopted around the notch tip, where the highest stress concentration was expected. A mesh sensitivity analysis, using the *sub-modelling* technique, confirmed the independence of the results from element size.

The net stress concentration factors on σ_1, based on stress values at nodes are reported in Table 2. The maximum extrapolated value was considered, without performing any averaging of the values deriving from contiguous elements.

Table 2. Orthotropic stress concentration factors for σ_1 from FEA, referring to the nominal net area

ρ [mm]	80	5	1	0.5	0.2
$K_{t1,n}$ [-]	1.16	2.84	5.58	7.82	11.67

The calculation of the control volume V_C and of the average SED was carried out by a post-processing python script for each specimen geometry. Given a material critical radius R_C, a notch radius ρ and opening angle 2α as input, the script records the elements and integration points of the specimen mesh falling in the control volume and returns the maximum and average values of the SED. The representation of V_C for two notch types are displayed in Fig. 3.

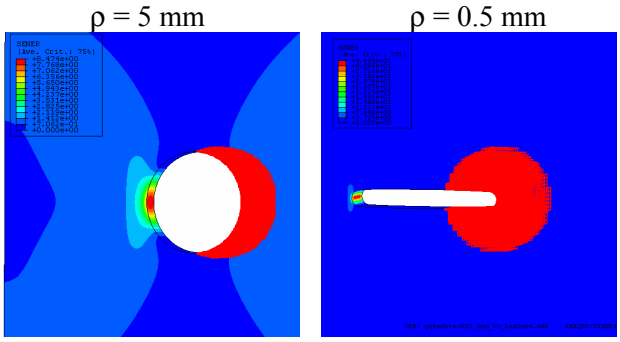

Fig. 3. Representation of the control volume V_C on a specimen with a central hole (left) and a specimen with a central slit (right)

Distances and volumes calculation was carried out on integration point coordinates and volumes instead of element centroid coordinates and element volumes, in order to achieve a better accuracy in the computation of ΔW_{avg} and V_C.

The shape of the control volume depends upon specimen geometry and must be properly chosen and implemented every time by the user. In this reanalysis a sector of a prism with circular cross-section was used, since the specimens are extrusion solids.

4 Modelling of fatigue data

In order to account for the fatigue strength reduction due to notches, different energetic formulations were considered. The fatigue data were rearranged in terms of distinct types of SED ranges, namely nominal SED, elastic peak SED and average SED over a control volume.

Fig. 4 and Fig. 7 show the nominal SED range ΔW_{nom} at RT for R = 0 and R = -1 respectively as a function of the number of cycles to failure N for the different notch geometries. ΔW_{nom} is computed entering the ranges of nominal applied stress components and the material compliance matrix components in equation (2), both referring to the geometrical coordinate system 0,X,Y,Z instead of the one of the material. No FEA is needed to plot these diagrams.

A significant decrease of ΔW_{nom} to failure with increasing the notch sharpness can be noticed. For notch radii ρ below 0.5 mm this reduction becomes marginal, indicating that an asymptotic ΔW_{nom} value exists. The data can not be compacted in a single scatter band using this variable.

Fig. 5 and Fig. 8, instead, show the fatigue data in terms of elastic peak SED range ΔW_{elpeak} at RT. The ΔW_{elpeak} were calculated as:

$$\Delta W_{elpeak} = \frac{W_{elpeak,\max}}{c_W} \qquad (9)$$

Where $W_{elpeak,max}$ is the maximal local value of SED resulting from a FEA when the maximum fatigue load within a cycle is applied to the specimen, and c_w is the load ratio parameter already introduced in equation (2).

The allowable elastic peak SED for sharp-notched specimens results significantly higher than the plain specimen one. Again the different curves can not be summarised in a single scatter band, indicating that the elastic stress concentration factors K_t are well above the fatigue strength reduction factors K_f at $N = 10^6$.

Fig. 6 and Fig. 9 present the average SED ranges ΔW_{avg} over a control volume V_C at RT. The control volume is defined by a control radius R_C, assumed to be a material characteristic length.

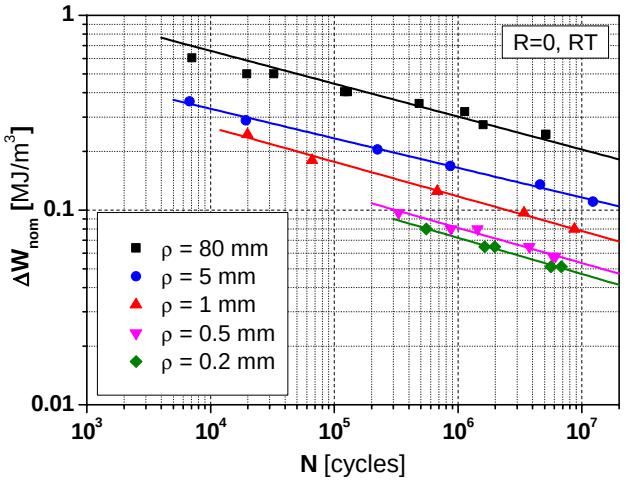

Fig. 4. Uniaxial fatigue data at RT, R=0 in terms of nominal SED range

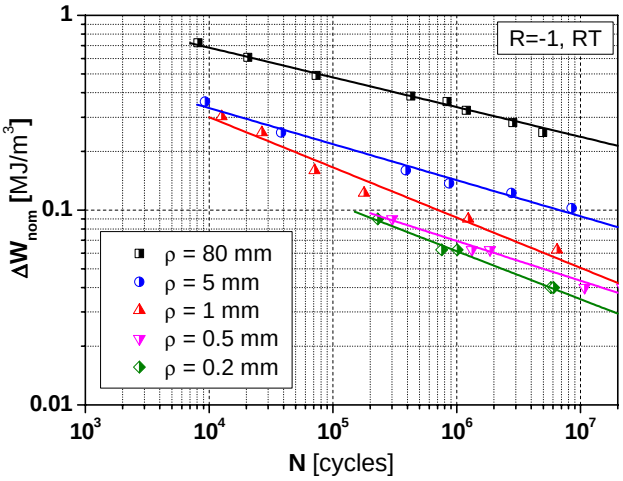

Fig. 7. Uniaxial fatigue data at RT, R=-1 in terms of nominal SED range

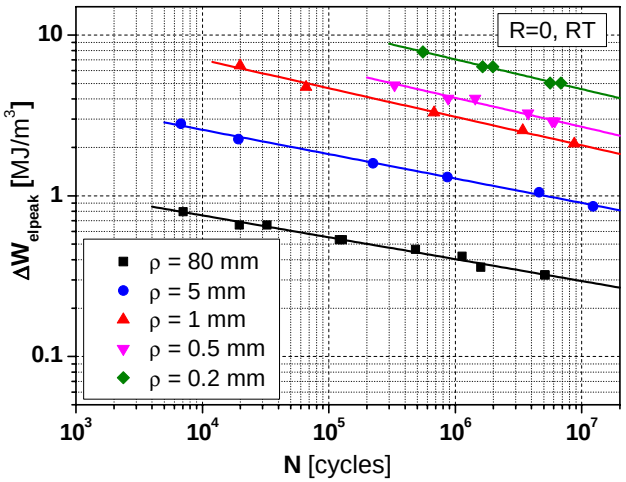

Fig. 5. Uniaxial fatigue data at RT, R=0 in terms of elastic peak SED range

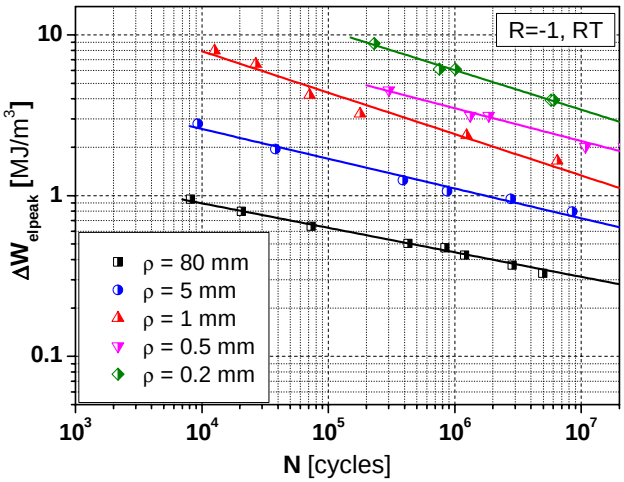

Fig. 8. Uniaxial fatigue data at RT, R=-1 in terms of elastic peak SED range

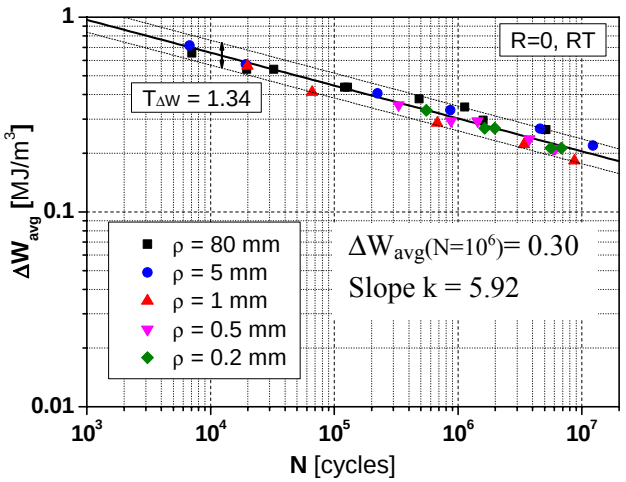

Fig. 6. Uniaxial fatigue data at RT, R=0 rearranged in terms of averaged SED range over a control volume (c_w = 1.0)

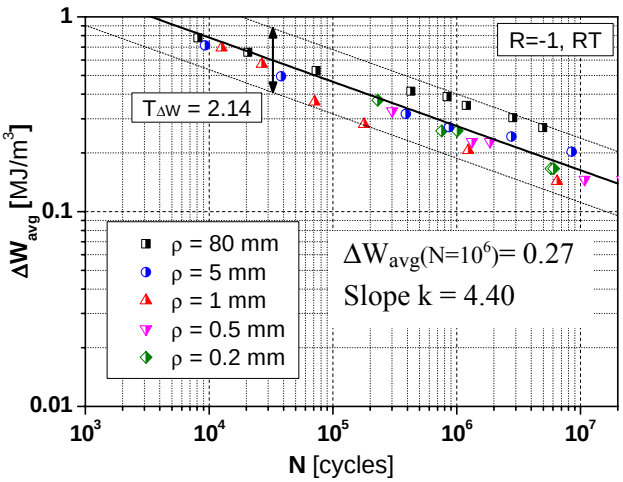

Fig. 9. Uniaxial fatigue data at RT, R=-1 rearranged in terms of averaged SED range over a control volume (c_w = 0.5)

R_C depends on fracture toughness, K_{IC} and ultimate tensile strength in case of static loading and on threshold behaviour ΔK_{th} and plain fatigue strength in case of cyclic loading. Since ΔK_{th} for the examined material was not available and anyway difficult to measure experimentally, we decided to determine R_C *a posteriori* as the radius providing, for the sharpest notch (ρ = 0.2 mm), an average SED on the control volume equal to the critical SED on the plain specimen ΔW_c at a reference number of cycles to failure $N = 10^6$. ΔW_c was computed as the average SED range value in the central part of the plain specimen (ρ = 80 mm) under application of the failure loading at $N = 10^6$. For R = 0 and RT R_C resulted equal to 3 mm; this value was afterwards applied to all other notch geometries and loading conditions (R = -1). Table 3 and Table 4 report the obtained average SED at RT, $N = 10^6$ cycles for the different notch radii.

Table 3. Averaged strain energy densities over V_C at N= 10^6, R = 0, RT (ΔW_c = 0.30 MJ/m^3)

ρ [mm]	$\Delta\sigma_{nom}$ [MPa]	ΔW_{avg} [MJ/m^3]	$\Delta W_{avg}/\Delta W_c$ [-]	V_C [mm^3]	Int. Pt.s [-]
80	78.37	0.3314	1.10	229.49	4480
5	57.37	0.3260	1.09	104.01	50024
1	48.48	0.2692	0.90	92.87	90288
0.5	40.19	0.2950	0.98	89.98	119728
0.2	37.95	0.2997	0.99	86.75	195712

Table 4. Averaged strain energy densities over V_C at N= 10^6, R = -1, RT (ΔW_c = 0.30 MJ/m^3)

ρ [mm]	$\Delta\sigma_{nom}$ [MPa]	ΔW_{avg} [MJ/m^3]	$\Delta W_{avg}/\Delta W_c$ [-]	V_C [mm^3]	Int. Pt.s [-]
80	58.13	0.3647	1.22	229.49	4480
5	37.73	0.2820	0.94	104.01	50024
1	30.25	0.2097	0.70	92.87	90288
0.5	26.35	0.2539	0.85	89.98	119728
0.2	24.80	0.2553	0.85	86.75	195712

The fatigue data at RT can be summarised within a single scatter band in terms of average SED range ΔW_{avg} as shown in Fig. 6 for R = 0 and in Fig. 9 for R = -1. Errors on response are assumed to be normally distributed with a constant variance (standard deviation). The number of data in every fitting was accounted by using the correction factor K_1 of one-sided tolerance limits for normal distributions proposed by Natrella [20]. The data scatter indexes $T_{\Delta W}$ refer to the ratio, at a given number of cycles, between the SED range value at 90% and the one at 10% failure probability: $T_{\Delta W} = \Delta W_{u,90\%} / \Delta W_{u,10\%}$. For R = 0 the scatter index is comparable to that obtained for each single series.

Fig. 10 displays all the 63 fatigue data points considered at RT, evidencing how five different notch geometries and two load ratios can be summarized in a unique scatter band.

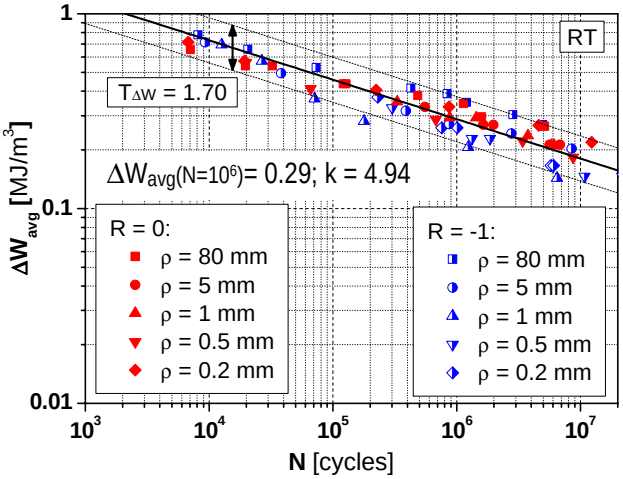

Fig. 10. Uniaxial fatigue data at RT rearranged in terms of averaged SED range over a control volume

Fig. 11 and Fig. 12 show the fatigue data at 130°C in terms of nominal SED for R = 0 and R=-1 respectively. Using the load ratio parameter c_W, the data can be even summarized in a unique scatter band (see Fig. 13). Evidently there is no need to use any notch accounting method like the elastic peak SED or the average SED to compact the data of different notch geometries: at 130°C the material appears in fact to be notch-insensitive. While at RT the material behaves in a brittle manner, as its cyclic behaviour is perfectly linear elastic, at T = 130°C the material is more ductile, showing noticeable non-linearity of the response, hysteresis area (damping) and plastic deformation. This marked difference in the constitutive response is due to the fact that RT is below the material glass transition temperature T_g = 65°C, while 130°C is well above T_g. Being the mobility of the polymeric chains much higher above T_g, they are able to stretch significantly under stress, allowing larger strains to be achieved.

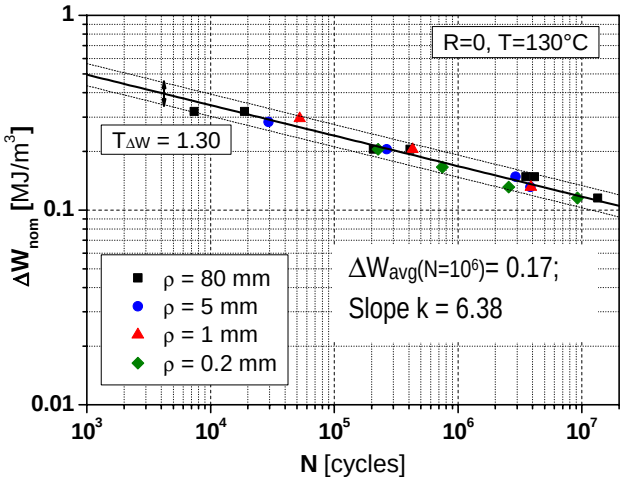

Fig. 11. Uniaxial fatigue data at T = 130°C, R=0 in terms of nominal SED range

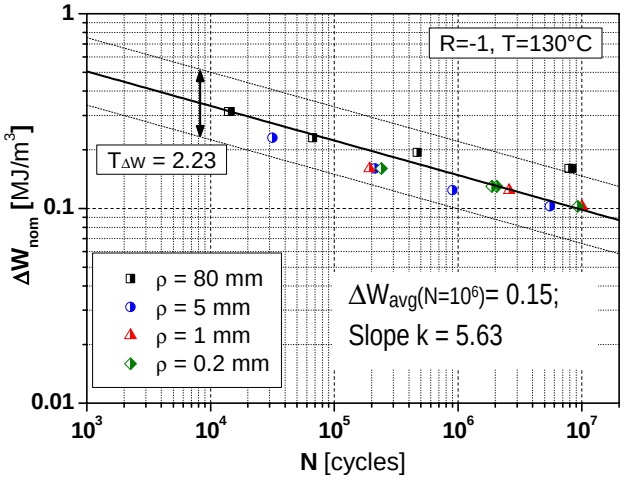

Fig. 12. Uniaxial fatigue data at T = 130°C, R = -1 in terms of nominal SED range

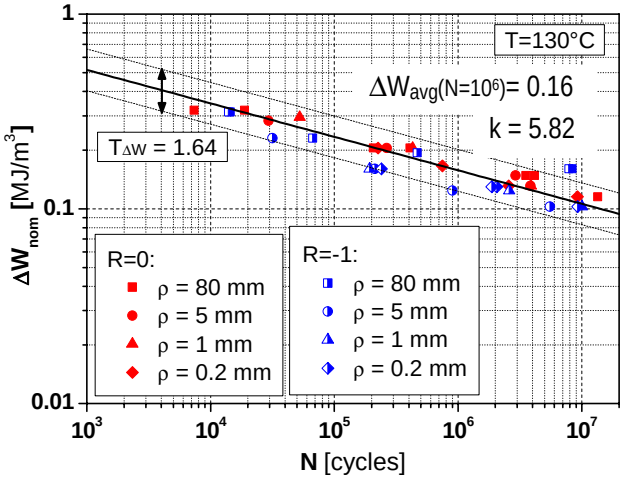

Fig. 13. Uniaxial fatigue data at T = 130°C in terms of nominal SED range

In conclusion, at temperatures higher than T_g the material changes completely its mechanical behaviour.

When applying the average SED criterion a larger control radius should be used in the definition of the control volume to account for the increased material ductility. In general it can be stated that the more ductily the material behaves the larger the critical radius will be.

5 Discussion

The proposed average SED criterion allows for an easy characterisation of the notch sensitivity under cyclic loading, since for a given material configuration it requires only two fatigue curves, namely on a plain specimen and on a severely notched or cracked one. A fatigue strength assessment on any other notch geometry can be afterwards performed, just paying some attention to the shape of the control volume. The testing effort required to transfer the material properties in the fatigue design from specimen to components is significantly reduced if compared to other conventional criteria commonly used in the failure assessment of metals as well as SFRP materials. Concepts like the support effect on bearable local stresses due to the stress gradient or the highly stressed volume [21], [22] require, indeed, a larger number of notch radii to be validated.

There are however some limitations to the application of average SED criterion. The main concern for injection moulded SFRP is to assure that the specimen or component considered has the same material configuration as those used to derive ΔW_c and R_C. The critical SED ranges at RT under uniaxial loading (R = 0) at an angle θ with respect to nominal fibre direction, calculated from the data reported in [16], were: ΔW_c = 0.30 MJ/m^3 for θ = 0°, ΔW_c = 0.29 MJ/m^3 for θ = 30° and ΔW_c = 0.21 MJ/m^3 for θ = 90°. These values confirm that fibre orientation plays an important role in determining the critical SED and consequently the material critical radius R_C.

Another limitation is that the criterion is not capable to account for different slopes at diverse notch radii or load ratios. Experimental data, instead, show that Wöhler curves become steeper (lower k value) by increasing notch sharpness. It must be also remarked that this criterion is valid only until the material remains locally in the linear elastic field. This is probably the reason for the considerable scatter displayed by the ΔW_{avg} data at 130°C. The

same problem was encountered trying to apply the criterion to the quasi-static strength data. The extension of the criterion to elasto-plastic and visco-elasto-plastic behaviour is still under investigation. In view of this limitation it is quite surprising that Zago and Springer [12] could use the d_0 value obtained from quasi-static strengths to fatigue strength data. However, with the data discussed in this paper the *Point Stress Criterion* did not allow for an assessment of the fatigue strength of the different notched specimens with a unique distance d_0.

Considering the scatter bands obtained with the average SED criterion, $T_{\Delta W}$ for R = 0 appears significantly narrower than for R = -1. At RT this is only partially due to the fact that R_C and ΔW_c were calculated referring to the data at R = 0. Re-calculating the two parameters R_C and ΔW_c on the R = -1 data it would result R_C = 1.9 mm and ΔW_c = 0.33 MJ/m^3; the scatter band values would become $T_{\Delta W}$ = 1.63 for R = 0 and $T_{\Delta W}$ = 1.81 for R = -1. Comparing the data at RT (Fig. 6 and Fig. 9) with the data at 130°C (Fig. 11 and Fig. 12) it can be noticed that the larger scatter at R = -1 is encountered at RT, where the average SED criterion is used, as well as at 130°C, where the nominal stresses are considered. Therefore, this effect should be connected intrinsically with the data rather than with the model chosen for the analysis; the reasons of such evidence are not clearly understood. Possible explanations for the larger scatter at R = -1 could be the presence of the anti-buckling device and the relative alignment of the testing machine clamps, which become more important when the specimen is under compression than under tensile loading. Nevertheless it is worth noting that the scatter index $T_{\Delta W}$ at R = -1 is of the same order of magnitude of the ones resulting from each single data series. The proposed criterion can thus be applied for every load ratio in the range -1 < R <0.

It is interesting that modelling the material as isotropic would not change significantly the results produced with the average SED criterion. Setting $E = E_1$ on the plain specimen (ρ = 80 mm) under application of the failure loading at $N = 10^6$, RT, R = 0, would generate ΔW_c = 0.34 MJ/m^3, with an error of 13% with respect to the transverse isotropic modelling. Even modelling the material as orthotropic, using some micromechanical model to compute the elastic constants, would not affect significantly the average SED values. It can be thus claimed that the criterion is quite robust to the type of material modelling chosen by the user, avoiding the necessity to carry out a full 3D characterization of the material response (at least in the preliminary design phase).

The size of the control radius R_C obtained for PA66-GF35 is considerably larger than typical control radii reported for metals (R_C = 0.1 ÷ 0.5 mm), indicating that the material is significantly more ductile and less notch sensitive than metals.

Noticeably R_C is far too large to be associated with any physical features of the material, i.e. average fibre length (l_{avg} = 280 µm), crystallites size (spherulites dimensions on PA66-GF35 are typically below 100 µm),…

Knowing R_C, a rough estimation of the threshold value ΔK_{th}, for the considered material and load configuration, can be made using eq. (5): for R = 0 at RT it results ΔK_{th} = 8.92 MPa m$^{0.5}$. This value is not congruent with the ΔK_{th} extrapolated from the Paris curves reported for similar materials in the same configuration by Zahnt [23] and Karger-Kocsis [24]. A reformulation of eq. (5) for orthotropic materials is thus desirable to better estimate the material critical radius from fracture mechanics.

6 Conclusions

In this paper we presented a reanalysis of fatigue strength data of different notched specimens made of PA66-GF35, in terms of average SED range over a control volume. The resulting fatigue failure criterion represents an extension to SFRP of the energetic approach proposed by Lazzarin *et al.* [1], [2], [6] for isotropic materials. The shape of the control volume depends upon specimen geometry and is defined by a material critical radius R_C. For orthotropic materials, R_C depends not only on plain fatigue strength and on threshold behaviour ΔK_{th}, as it is the case for isotropic materials, but also on the loading configuration with respect to the material axis. Moreover, for SFRP the testing temperature should be considered, being aware of the fact that the proposed criterion is valid only in the linear elastic field. The application of the proposed energetic criterion requires only two fatigue curves to be calibrated and can be afterwards employed for every other notch radius. The fatigue curve of an unnotched specimen is required to determine the critical SED range ΔW_c and the fatigue curve of a severely notched or cracked specimen allow to infer the material critical radius R_C.

For PA66-GF35 at RT, with nominal fibre direction aligned with the loading axis, we found out that ΔW_c = 0.30 MJ/m^3 and R_C = 3 mm.

Using these parameters, all the fatigue data at RT, including five different notch radii and two load ratios could be compacted in a narrow scatter band.

In general it is believed that averaging the SED over a small volume around the critical area in the component, usually a transition radius, can provide a way to compare the stress state in the component to that of plain testing specimens.

At 130°C, instead, the criterion could not be applied since the material shows a non-linear response even in the high cycle fatigue region. In particular, the material appeared to be notch insensitive at temperature higher than its T_g.

The average SED range criterion resulted a useful tool in the structural durability evaluation of injection moulded components at RT already in the design phase.

References

[1] P. Lazzarin, R. Zambardi. "A finite-volume-energy based approach to predict the static and fatigue behavior of components with sharp V-shaped notches". *International Journal of Fracture*, 112 (3), pp. 275-298, 2001

[2] B. Atzori, F. Berto, P. Lazzarin, M. Quaresimin. "Multi-axial fatigue behaviour of severely notched carbon steel". *Int. J. Fatigue*, 28 (2006), pp. 485-493

[3] F. Ellyin, H. El-Kadi. "A fatigue failure criterion for fibre reinforced composite laminae". *Composite Structures*, 15, 1990, pp. 61-74

[4] Yosibash, Z., Bussiba, A.R and Gilad, I. "Failure criteria for brittle elastic materials", *Int. J. Fracture*, 125 (2004), pp. 307–333

[5] Neuber, H. (1958) "*Theory of Notch Stresses*", Springer-Verlag, Berlin

[6] P. Lazzarin, F. Berto. "Some expressions for the strain energy in a finite volume surrounding the root of blunt notches". *Int. J. Fracture*, 135 (2005), pp. 161-185

[7] J.M. Whitney, R.J. Nuismer, "Stress Fracture Criteria for Laminated Composites Containing Stress Concentrations". *J. of Composite Materials*, 8 (1974); pp. 253-265

[8] R.J. Nuismer, J.M. Whitney, "Uniaxial Failure of Composite Laminates Containing Stress Concentrations". *Fracture Mechanics of Composites ASTM STP 593*, pp. 117-142, 1975

[9] S.C. Tan, "Laminated composites containing an elliptical opening. I. Approximate stress analyses and fracture models", *J. Composite Materials*, 21, pp. 925-948, 1987

[10] S.C. Tan, "Laminated composites containing an elliptical opening. II. Experiment and model verification", *J. Composite Materials*, 21, pp. 949-968, 1987

[11] S.C. Tan, "Finite-width correction factors for anisotropic plate containing a central opening", *J. Composite Materials*, 22, pp. 1081-1097, 1988

[12] A. Zago, G.S. Springer "Fatigue live of short glass fibre reinforced thermoplastics parts", *Journal of Reinforced Plastics and Composites*, 20 (7), pp. 606-620, 2001

[13] P. Lazzarin, R. Tovo, "A unified approach to the evaluation of linear elastic stress fields in the neighbourhood of cracks and notches", *Int. J. Fracture*, 78 (1996), pp. 3-19

[14] P. Lazzarin, C.M. Sonsino, R. Zambardi, "A notch stress intensity approach to assess the multiaxial fatigue strength of welded tube-to flange joints subjected to combined loadings", *Fatigue Fract Eng Mater Struct* 2004 (27), pp.127–140

[15] E. Moosbrugger, R. Wieland, P. Gumnior and J.J. Gerharz, "Design and dimensioning of high loaded plastic parts in engine compartments", *Material Testing* 47 (7-8), 2005 (in German)

[16] M. De Monte, E. Moosbrugger, M. Quaresimin, "Influence of temperature and thickness on static and cyclic off-axis behaviour of short glass fibre reinforced polyamide 6.6", *Proceedings of XXXV AIAS Conference*, Ed. CRACE - Università Politecnica delle Marche, 13-16 September 2006, Ancona (Italy), pp. 115-116

[17] R. M. Christensen, "The number of elastic properties and failure parameters for fibre composites", *Journal of Engineering Materials and Technology*, 120, 1998, pp. 110-113

[18] J.M. Berthelot, *Composite Materials*, Springer Verlag, New York, 1999

[19] ABAQUS Documentation Vers. 6.5 - Analysis User Manual, ABAQUS Inc., 2004

[20] M.G. Natrella, "Experimental statistics", Handbook 91, National Bureau of Standards; 1966, pp. 2-15

[21] R. Kuguel, "A Relation between Theoretical Stress Concentration Factor and Fatigue Notch Factor Deducted from the Concept of Highly Stressed Volume", *ASTM STP Proc.* 61 (1961), pp. 732-748

[22] C.M. Sonsino, "Evaluating the Fatigue Behaviour of Components with Consideration of Local Stresses", *Konstruktion* 45 (1993), pp. 25 – 33 (in German)

[23] B.A. Zahnt, "*Fatigue behaviour of discontinuous glass fiber reinforced plastics*", Ph.D. Thesis, Montanuniversität Leoben (Austria), 2003 (in German)

[24] J. Karger-Kocsis, K. Friedrich, "Skin-core morphology and humidity effects on the fatigue crack propagation of PA-6.6", *Plastics and Rubber Processing and Applications*, 12 (1989), pp. 63-68